

Electronic supplementary information (ESI)

Highly active and stable 3D dandelion spore-structured self-supporting Ir-based electrocatalyst for proton exchange membrane water electrolysis fabricated using structural reconstruction

Kyeong-Rim Yeo^a, Kug-Seung Lee^b, Hoyoung Kim^{*, c}, Jinwoo Lee^{*, c}, Soo-Kil Kim^{*, a}

^a School of Integrative Engineering, Chung-Ang University, 84 Heukseok-ro, Dongjak-gu, Seoul 06974, Republic of Korea

^b Pohang Accelerator Laboratory, 80 Jigok-ro, Nam-gu, Pohang 37673, Republic of Korea

^c Department of Chemical and Biomolecular Engineering, Korea Advanced Institute of Science and Technology (KAIST), 291 Daehak-ro, Yuseong-gu, Daejeon 34141, Republic of Korea

Correspondence and requests for materials should be addressed to S.-K.K. (email: sookilkim@cau.ac.kr), J. Lee (email: jwlee1@kaist.ac.kr) or H. Kim (email: town57@naver.com)

Table S1. Combination of membrane electrode assemblies for single-cell operation.

Membrane Electrode Assembly (MEA)				
Cathode (Loading amount)	gasket	Membrane	gasket	Anode (Loading amount)
Pt/C (0.4 mg _{Pt} cm ⁻²)	250	Nafion® 212	250	Com. IrO _x (Ti) (0.7 mg _{Ir} cm ⁻²)
	250			Com. IrO _x (Ti) (2 mg _{Ir} cm ⁻²)
	250		DNP-IrNi (Ti)	
	250		215	Com. IrO _x (CP) (0.7 mg _{Ir} cm ⁻²)
	250			Com. IrO _x (CP) (2 mg _{Ir} cm ⁻²)
	215		DNP-IrNi (CP)	
DNP-IrNi (Ti)	250		250	DNP-IrNi (Ti)
DNP-IrNi (CP)	215		215	DNP-IrNi (CP)

Table S2. Compositions of ED-IrNi, DNP-IrNi, and DNP-IrNi after durability test measured by EDS, XPS and ICP-OES.
(Numbers with * denote composition without considering oxygen)

ED-IrNi	Ir	Ni	O
EDS atomic %	5.3*	94.7*	
	5.2	93.5	1.3
XPS atomic %	20.2*	79.8*	
	6.5	25.5	68
DNP-IrNi	Ir	Ni	O
EDS atomic %	84.8*	15.2*	
	59.8	10.6	29.6
XPS atomic %	90.5*	9.5*	
	26.7	2.8	70.5
ICP atomic %	87.2	12.8	
After durability of DNP-IrNi (at 100 mA cm ⁻² for 50 hours)	Ir	Ni	O
EDS atomic %	92.6*	7.4*	
	61.8	5	33.2
XPS atomic %	91.9*	8.1*	
	23.3	2	74.7
ICP atomic %	91.0	9.0	

Table S3. Comparison of OER activity and stability of DNP-IrNi with literature-reported Ir-based electrocatalysts and the corresponding conditions in acidic electrolytes.

Catalyst	Overpotential @10 mA cm ⁻²	Tafel slope (mV dec ⁻¹)	Mass loading (Ir)	Substrate	Electrolyte	Stability	Reference
DNP-IrNi	248 mV	38	0.67 mg cm ⁻²	Ti fiber felt	0.5 M H ₂ SO ₄	50 h @ 100 mA cm ⁻² 50 h @ 200 mA cm ⁻² 1.2 - 1.6 V _{RHE} @ 5k cycles	This work
IrO ₂ @Mn-5	275 mV	59	0.2 mg cm ⁻²	Ti plate	0.1 M HClO ₄	24 h @ 10 mA cm ⁻²	ACS Appl. Mater. Interfaces, 2017, 9, 41855.
IrW	305 mV	56.6	10.2 µg cm ⁻²	GC	0.5 M H ₂ SO ₄	8 h @ 10 mA cm ⁻²	ACS Cent. Sci. 2018, 4, 1244-1252.
IrNiCo	285 mV	53	0.2 mg cm ⁻²	Ti plate	0.1 M HClO ₄	5.5 h @ 10 mA cm ⁻²	ACS Energy Lett. 2017, 2, 2786.
Ir ₃ Cu aerogels	298 mV	47.4	N/A	GC	0.1 M HClO ₄	12 h @ 5 mA cm ⁻²	ACS Energy Lett. 2018, 3, 9, 2038.
Co-IrCu ONC/C	293 mV	50	20 µg cm ⁻²	GC	0.1 M HClO ₄	2 k cycles @ 1.2 -1.7 V	Adv. Funct. Mater. 2017, 27, 1604688.
IrNi NCs	280 mV	N/A	12.5 µg cm ⁻²	GC	0.1 M HClO ₄	120 h @ 5 mA cm ⁻²	Adv. Funct. Mater. 2017, 27, 1700886.
IPN cage/C	333 mV	57.4	10.2 µg cm ⁻²	GC	0.1 M HClO ₄	5 h @ 5 mA cm ⁻²	Adv. Funct. Mater. 2020, 30, 2003935.
IrO ₂ NN-L	313 mV	57	0.25 mg cm ⁻²	GC	1 M H ₂ SO ₄	2 h @ 10 mA cm ⁻²	Adv. Funct. Mater. 2018, 28, 1704796.
IrCoNi PHNC	303 mV	53.8	10 µg cm ⁻²	GC	0.1 M HClO ₄	200 min @ 5 mA cm ⁻²	Adv. Mater. 2017, 29, 1703798.
IrO ₂ /GCN	276 mV	57	81 µg cm ⁻²	GC	0.5 M H ₂ SO ₄	4 h @ 20 mA cm ⁻²	Angew. Chem. Int. Ed., 2019, 58, 12540
Ni _{0.34} Co _{0.46} Ir _{0.2} O _δ	280 mV	40.4	0.2 mg cm ⁻²	Ti plate	0.1 M HClO ₄	25 h @ 10 mA cm ⁻²	Appl. Catal. B, 2019, 244, 295–302.
Cu _{0.3} Ir _{0.7} Ox	351 mV	63	0.2 mg cm ⁻²	Ti plate	0.1 M HClO ₄	5.5 h @ 10 mA cm ⁻²	Chem. Sci. 2015, 6, 4993-4999.
IrNiFe	284 mV	48.6	92 µg cm ⁻²	GC	0.5 M HClO ₄	5.5 h @ 10 mA cm ⁻²	J. Mater. Chem. A 2017, 5, 24836.
Ir/VG	300 mV	59	N/A	GC	0.5 M H ₂ SO ₄	24 h @ 10 mA cm ⁻²	J. Mater. Chem. A 2019, 7, 20590.
Ir/GF	290 mV	46	0.82 mg cm ⁻²	Graphite foam	0.5 M H ₂ SO ₄	10 h @ 10 mA cm ⁻²	Nano Energy, 40, 2017, 27–33.
Ir-Ag nanotubes	285 mV	61.1	13.3 µg cm ⁻²	GC	0.5 M H ₂ SO ₄	6 h @ 5 mA cm ⁻²	Nano Energy, 56, 2019, 330-337.
Ir@N-G-750	303 mV	50	23 µg cm ⁻²	GC	0.5 M H ₂ SO ₄	20 h @ 20 mA cm ⁻²	Nano Energy, 62, 2019, 117-126.
IrNi NFs	293 mV	47.3	10.2 µg cm ⁻²	GC	0.1 M HClO ₄	1 k cycles @ 1.35-1.7 V 4h @ 20 mA cm ⁻²	Small Methods, 2020, 4, 1900129

Table S4. Comparison of DNP-IrNi with literature-reported results as a bifunctional catalyst in acidic media.

Catalyst	Electrolyte	Mass loading (mg cm ⁻²)	η at corresponding j (mV@ mA cm ⁻²)		Tafel slope (mV dec ⁻¹)		Reference
			HER	OER	HER	OER	
DNP-IrNi	0.5 M H ₂ SO ₄	0.67	17 @ 10	248 @ 10	28	38	This work
IrW	0.1 M HClO ₄	0.01	12 @ 10	305 @ 10	23.3	56.6	ACS Cent. Sci. 2018, 4, 1244-1252
CC/NPC/CP	0.5 M H ₂ SO ₄	N/A	100 @ 20	360 @ 20	60	N/A	ACS Sustainable Chem. Eng. 2017, 5, 571-579;
IrNi NCs	0.1 M HClO ₄	0.0125	19 @ 20	280 @ 10	N/A	N/A	Adv. Funct. Mater. 2017, 27, 1700886
Ni/Ru-doped Pt@Ni/Pt-doped RuO ₂	0.1 M HClO ₄	0.014	29.6 @ 10	239 @ 10	35	52	Adv. Mater. 2019, 31, 1805546
IrCoNi	0.1 M HClO ₄	0.01	33 @ 10	303 @ 10	37.9	53.8	Adv. Mater. 2017, 29, 1703798;
PdCu/Ir/C	0.1 M HClO ₄	0.0102	27 @ 10	283 @ 10	N/A	59.6	Angew. Chem., 2021, 133, 8324-8331
Ir NPs	0.1 M HClO ₄	0.09	17 @ 10	290 @ 10	51.4	32.8	Chem. Front. 2018, 5, 1121-1125
ONPPGC/OCC	0.5 M H ₂ SO ₄	0.1	386 @ 10	470 @ 10	109	200	Energy Environ. Sci. 2016, 9, 1210- 1214;
IrNiFe	0.5 M HClO ₄	0.092	24 @ 10	284 @ 10	34.6	48.6	J. Mater. Chem. A 2017, 5, 24836-24841.
PtNi/CNFs	0.5 M H ₂ SO ₄	N/A	34 @ 10	451 @ 10	31	198	J. Mater. Sci. 2017, 52, 13064-13077
Ir/GF	0.5 M H ₂ SO ₄	0.82	7 @ 10	290 @ 10	30	46	Nano Energy 2017, 40, 27-33
Ir NWs	0.1 M HClO ₄	0.031	11.3 @ 10	290 @ 10	29.8	43.6	Nanoscale 2018, 10, 1892-1897.
ACIN-HF	0.1 M HClO ₄	0.01	13.7 @ 10	308 @ 10	22	58	Nanoscale Horiz., 2019, 4, 727-734
IrNi NFs	0.1 M HClO ₄	0.0102	25 @ 10	293 @ 10	29.7	47.3	Small Methods, 2020, 4, 1900129

Table S5. PEMWE performance comparison; DNP-IrNi electrodes vs. literature-reported Ir-based anode.

Anode (Loading amount)	Membrane Electrode Assembly		Temperature (°C)	Current density (A cm ⁻² @ 1.7 V)	Cell voltage (V _{cell})		Reference
	Membrane	Cathode (Loading amount)			@ 1 A cm ⁻²	@ 2 A cm ⁻²	
DNP-IrNi/CP (0.67 mg _{Ir} cm ⁻²)	Nafion 212	DNP-IrNi/CP (0.67 mg _{Ir} cm ⁻²)	90	2.24	1.585	1.679	This work
DNP-IrNi/Ti (0.67 mg _{Ir} cm ⁻²)	Nafion 212	DNP-IrNi/Ti (0.67 mg _{Ir} cm ⁻²)	90	1.61	1.612	1.752	This work
DNP-IrNi/CP (0.67 mg _{Ir} cm ⁻²)	Nafion 212	Pt/C (0.4 mg _{Pt} cm ⁻²)	90	1.88	1.6	1.71	This work
DNP-IrNi/Ti (0.67 mg _{Ir} cm ⁻²)	Nafion 212	Pt/C (0.4 mg _{Pt} cm ⁻²)	90	1.42	1.623	1.794	This work
Ir _{0.7} Ru _{0.3} O _x (1.5 mg cm ⁻²)	Nafion 115	Pt/C (0.5 mg _{Pt} cm ⁻²)	90	1.884	1.569	1.716	Appl. Catal. B-Environ. 2015, 164, 488-495
IrO ₂ @TiO ₂ (1.2 mg _{Ir} cm ⁻²)	Nafion 212	Pt/C (0.5 mg _{Pt} cm ⁻²)	80	1.808	1.621	1.717	Appl. Catal. B-Environ. 2020, 269, 118762
Nanoporous gold/IrO ₂ (0.07 mg _{IrO2} cm ⁻²)	Nafion 212	Pt/C (1.0 mg _{Pt} cm ⁻²)	80	1.758	1.609	1.728	J. Power Sources 2017, 342, 947-955
IrO ₂ (0.1 mg _{Ir} cm ⁻²)	Nafion 212	Pt/C (0.4 mg _{Pt} cm ⁻²)	90	1.526	1.597	1.826	Appl. Catal. B Environ. 2015, 179, 285–291.
IrO ₂ inverse-opal (0.02 mg _{Ir} cm ⁻²)	Nafion 212	Pt/C (0.4 mg _{Pt} cm ⁻²)	90	1.302	1.635	1.907	Nano Energy 2019, 58, 158-166
Ir _{0.7} Ru _{0.3} O _x (1.8 mg cm ⁻²)	Nafion 115	Pt/C (0.5 mg _{Pt} cm ⁻²)	80	1.213	1.656	1.850	Adv. Energy Mater. 2019, 9, 1802136
Ir-nanodendrites/ATO (1.0 mg _{Ir} cm ⁻²)	Nafion 212	Pt/C (0.4 mg _{Pt} cm ⁻²)	80	1.115	1.670	1.916	Chem. Sci. 2015, 6, 3321
IrO ₂ (0.71 mg _{Ir} cm ⁻²)	Nafion 115	Pt/C (0.25 mg _{Pt} cm ⁻²)	80	0.966	1.708	1.928	Appl. Catal. B-Environ. 2016, 182, 153-160
IrO ₂ /Ti (0.12 mg _{Ir} cm ⁻²)	Nafion 115	Pt/C (0.25 mg _{Pt} cm ⁻²)	80	0.892	1.724	1.939	Appl. Catal. B-Environ. 2016, 182, 123
Ir/TiO ₂ -MoO _x (0.5 mg _{Ir} cm ⁻²)	Nafion 115	Pt/C (0.5 mg _{Pt} cm ⁻²)	80	0.845	1.740	1.872	Appl. Catal. B-Environ. 2021, 280, 119433

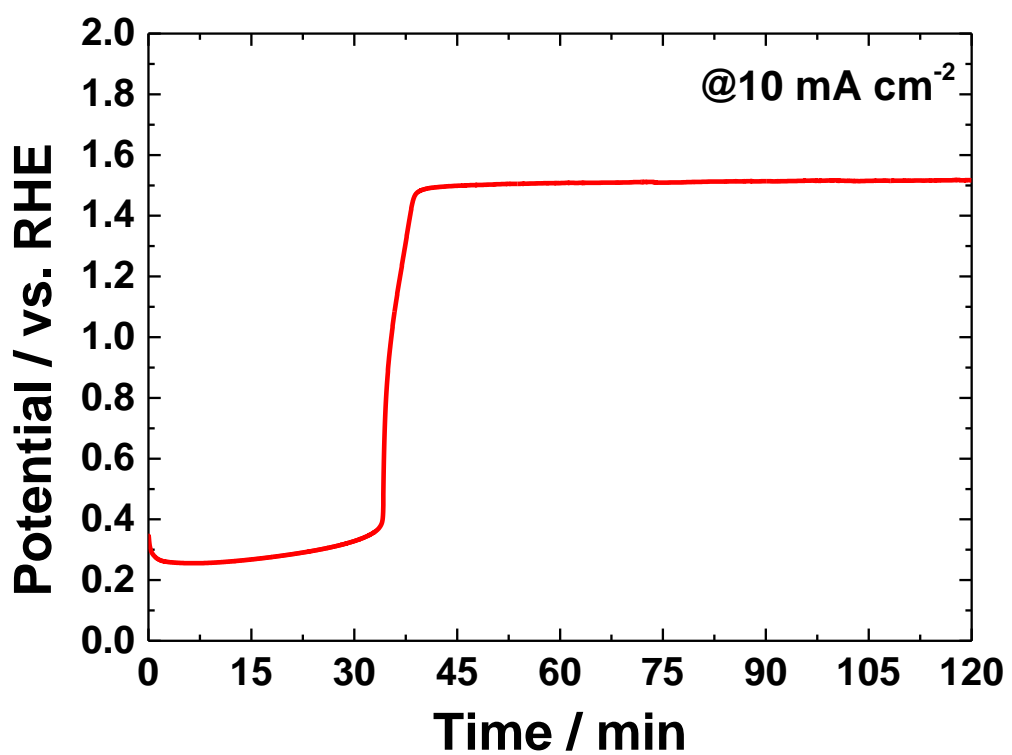


Figure S1. Chronopotentiometry curve during the de-alloying of ED-IrNi.

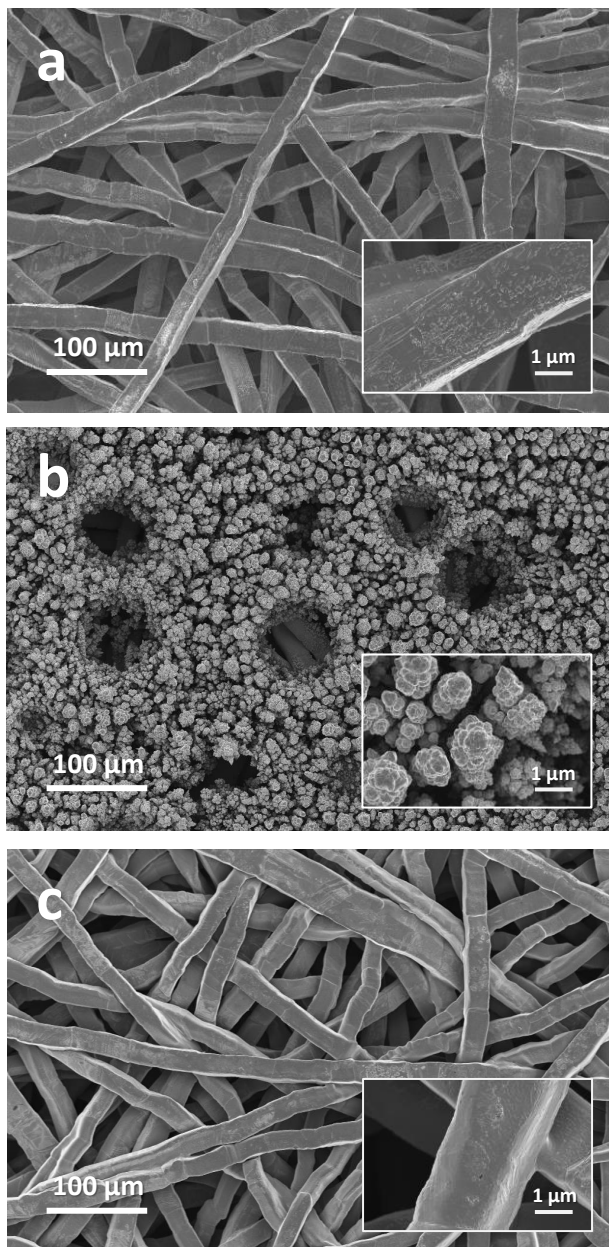


Figure S2. FE-SEM images of (a) pretreated Ti fiber felt, (b) Ni_{100} , (c) Ir_{100} ; The insets show the FE-SEM images at higher magnification.

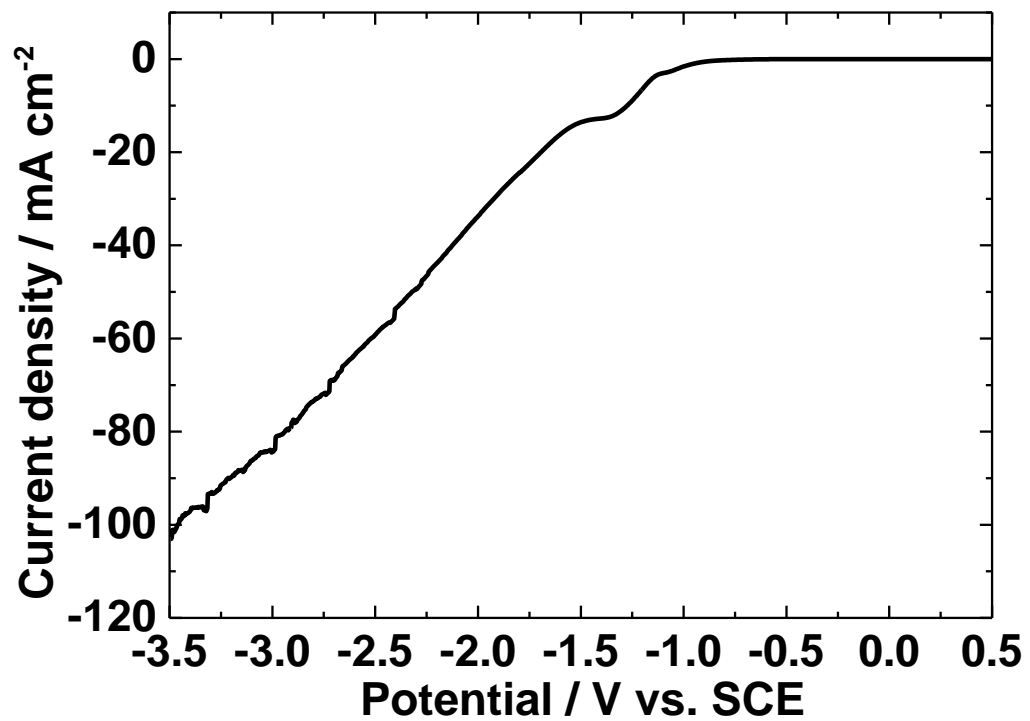


Figure S3. Linear sweep voltammetry in the Ni deposition electrolyte.

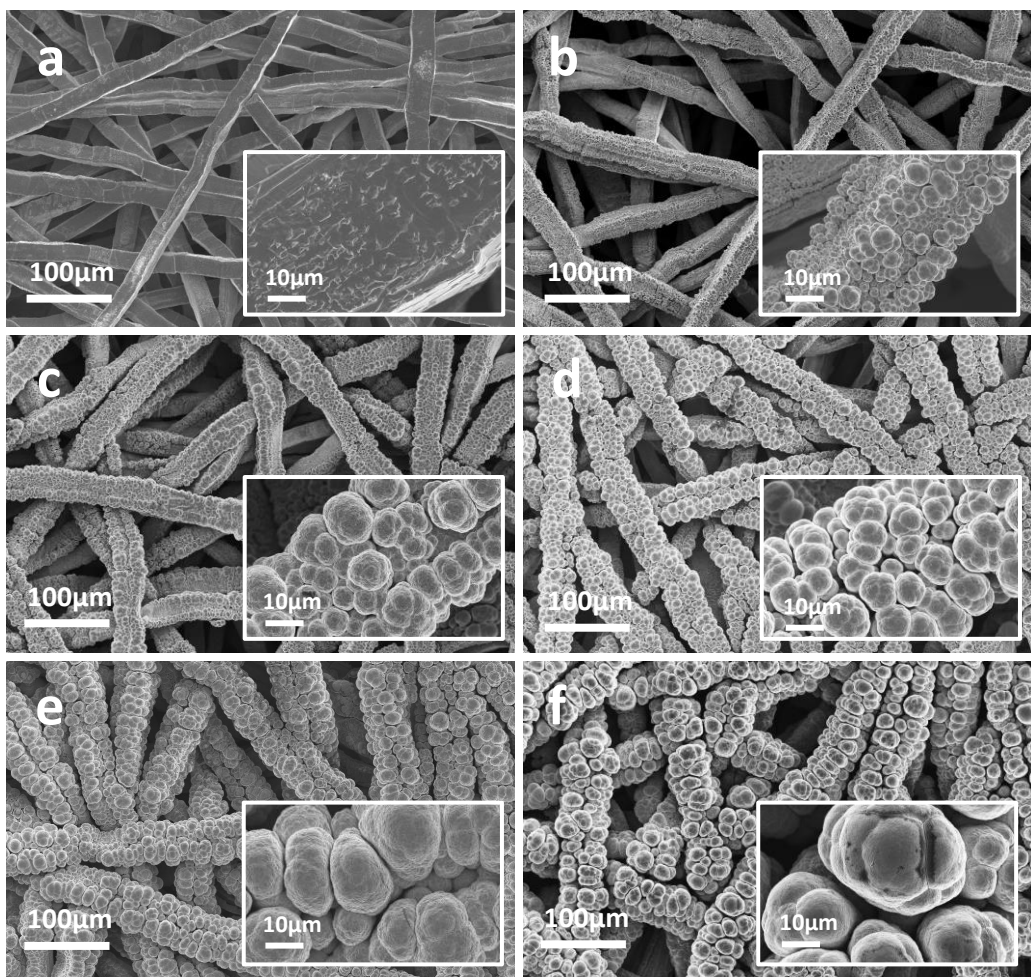


Figure S4. FE-SEM images of (a) pretreated Ti fiber and ED-IrNi deposits prepared at $-2.8\text{ V}_{\text{SCE}}$ for deposition time of (b) 5 min, (c) 10 min, (d) 15 min, (e) 30 min, and (f) 60 min. Inset shows FE-SEM images at higher magnification.

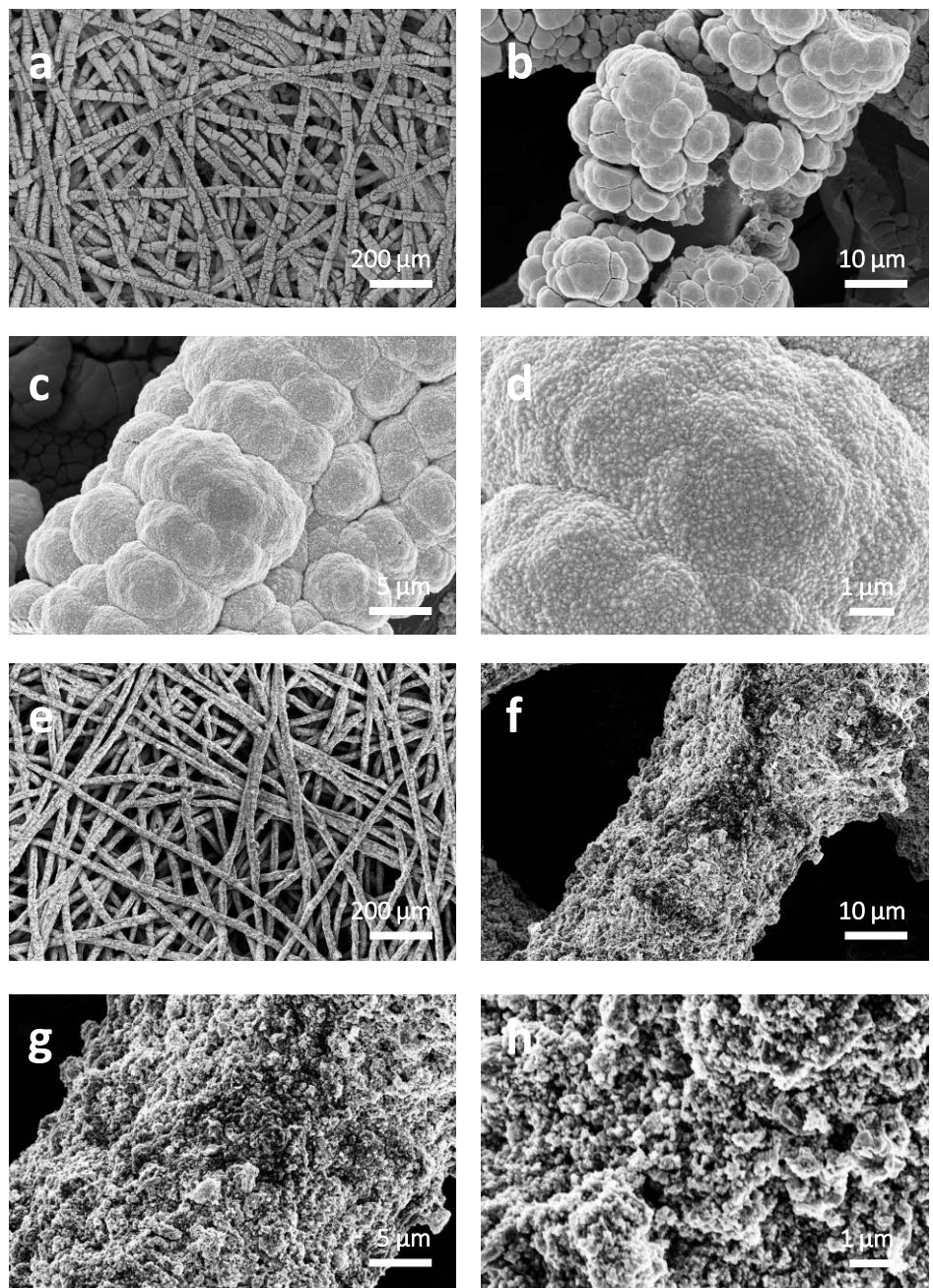


Figure S5. FE-SEM images of (a-d) HDNP-IrNi and (e-h) spray-coated Com. IrO_x at different magnification.

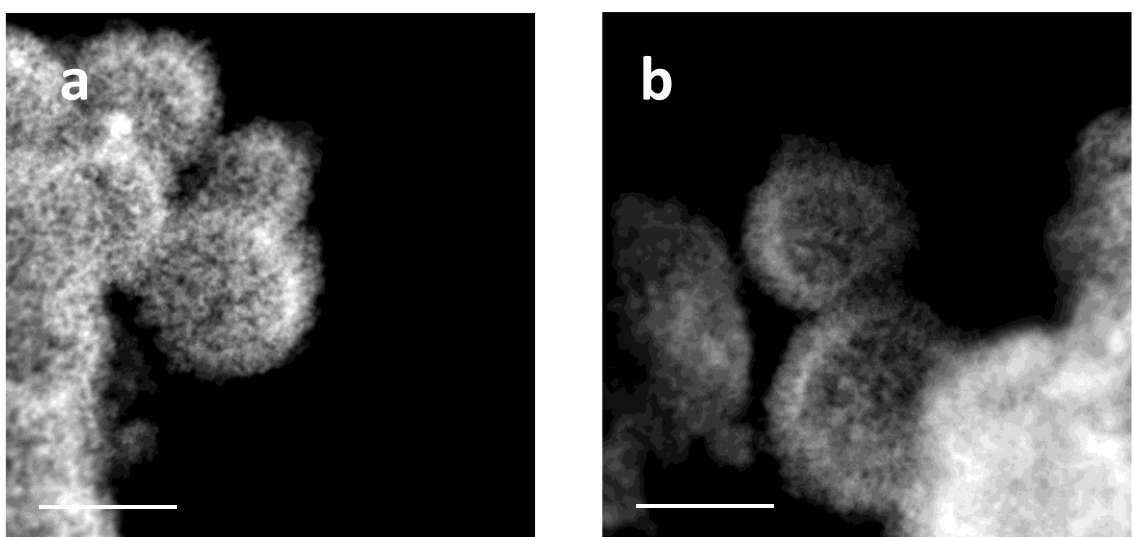


Figure S6. STEM images of DNP-IrNi at different sections.

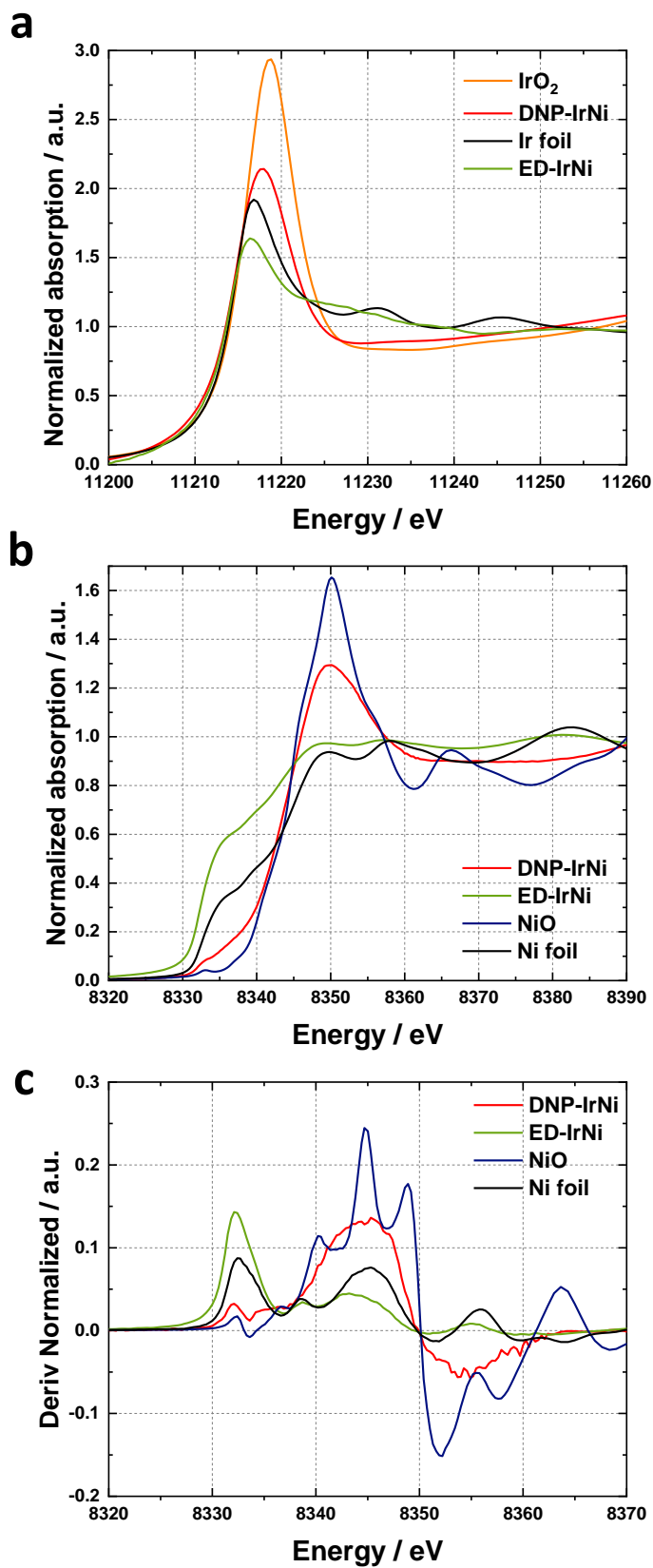


Figure S7. (a) Ir XANES, (b) Ni XANES, and (c) Derivation graph from (b)

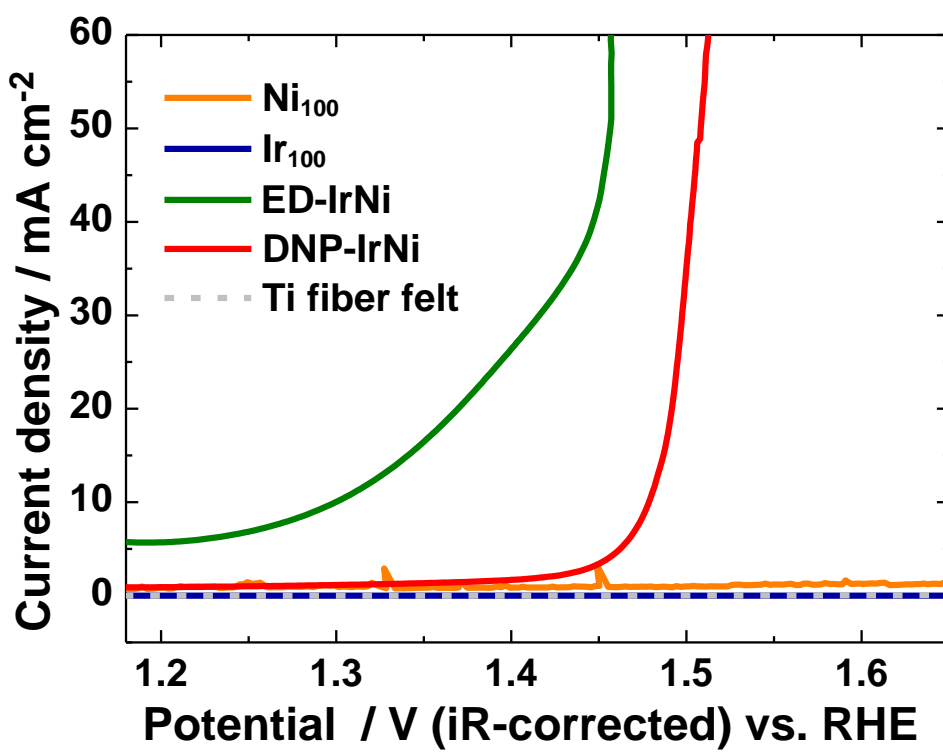


Figure S8. OER polarization curves of Ni_{100} , Ir_{100} , ED-IrNi, DNP-IrNi, and Ti fiber felt (substrate) measured at a scan rate of 1 mV s^{-1} with iR-compensation.

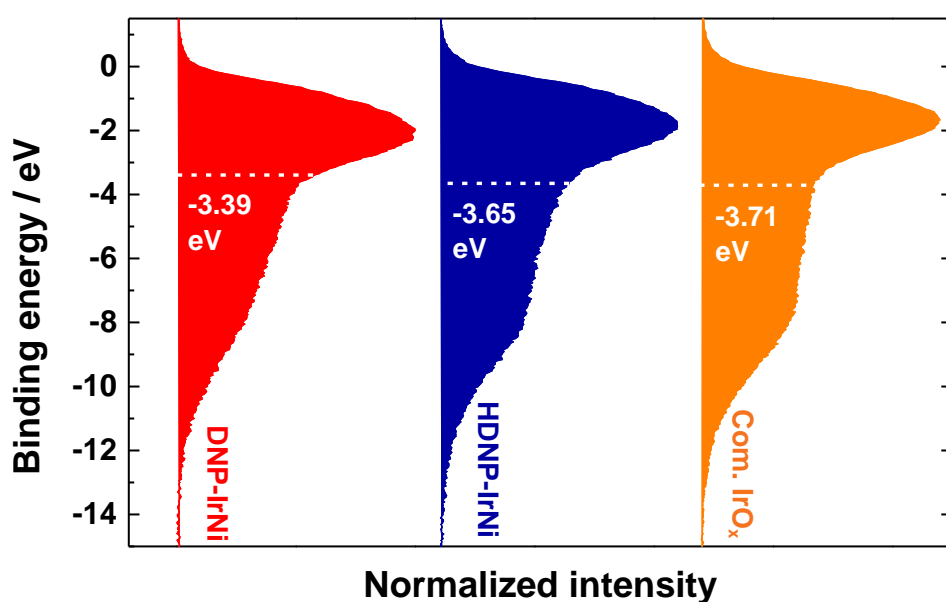


Figure S9. d-band center position experimentally estimated from the normalized valence band spectra (VBS) of DNP-IrNi, HDNP-IrNi, and Com. IrO_x.

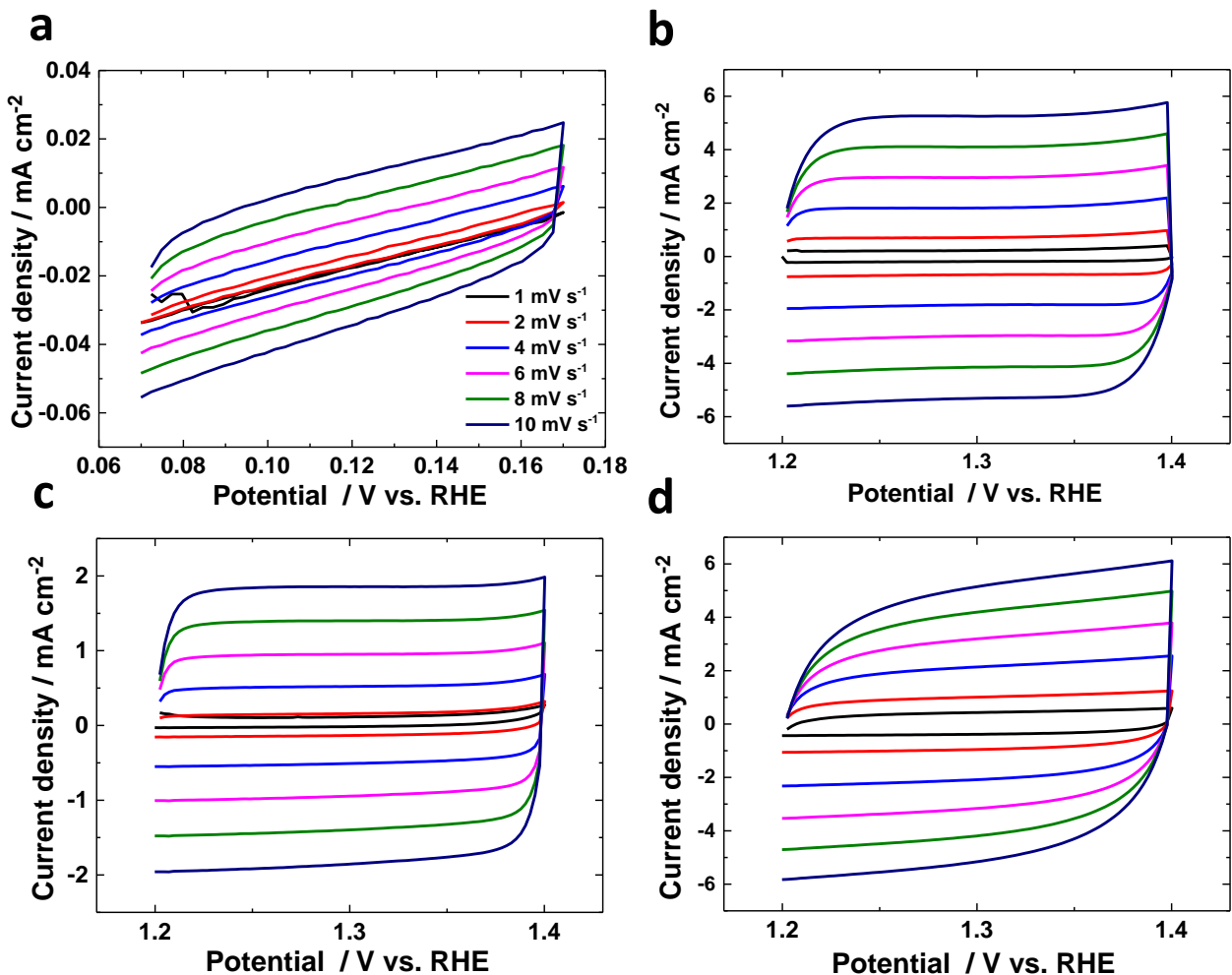


Figure S10. Measurements of electrochemical double layer capacitance of (a) pretreated Ti substrate, (b) DNP-IrNi, (c) HDNP-IrNi, and (d) Com. IrO_x .

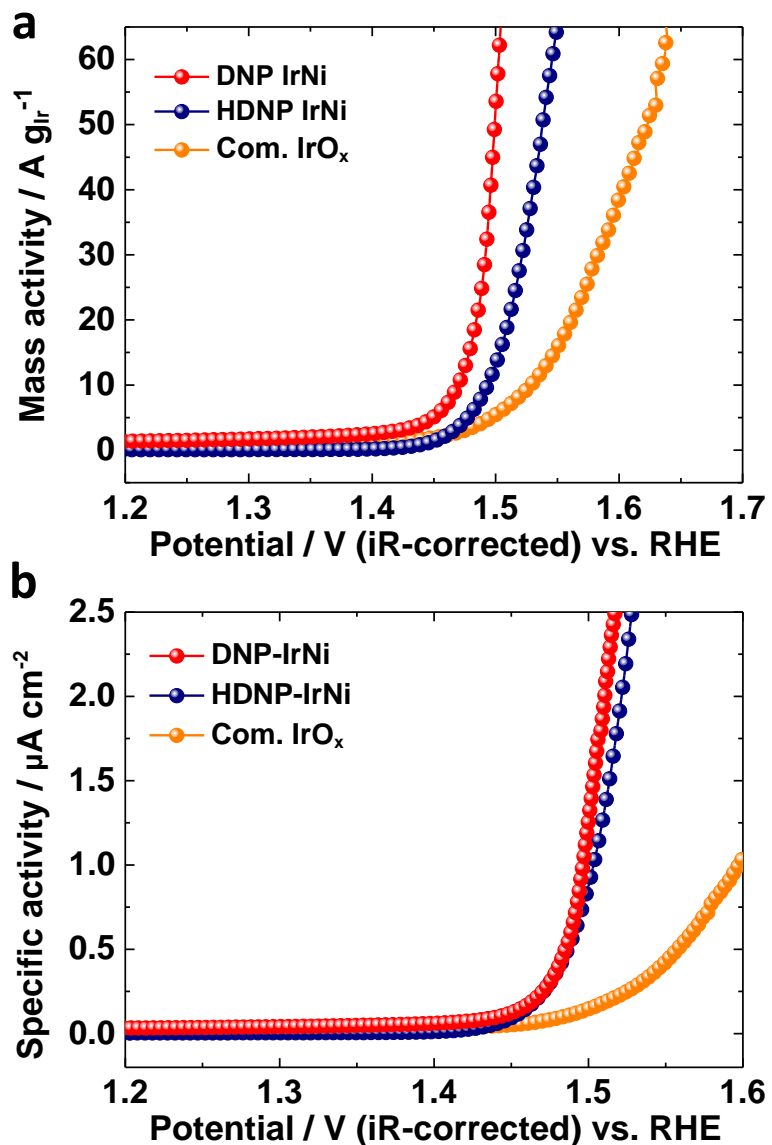


Figure S11. (a) Mass activity and (b) specific activity of DNP-IrNi, HDNP-IrNi, and Com. IrO_x .

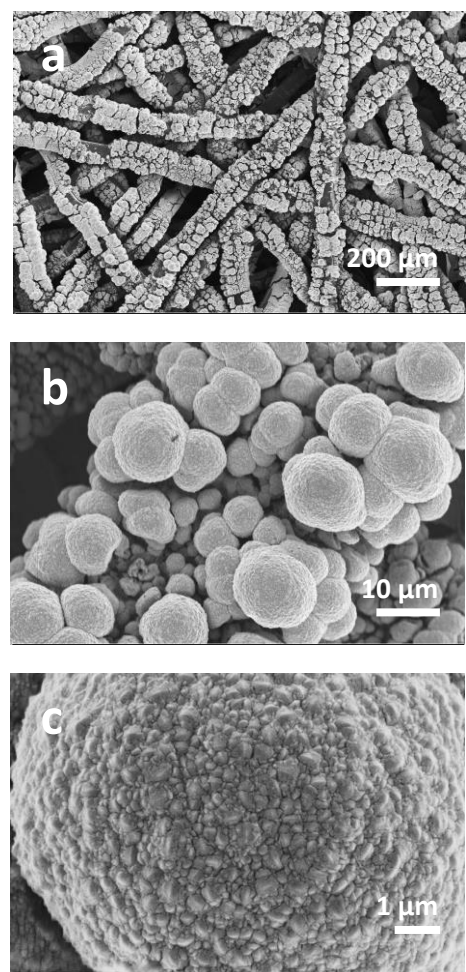


Figure S12. FE-SEM images of DNP-IrNi after applying a constant current density of 100 mA cm^{-2} for 50 h.

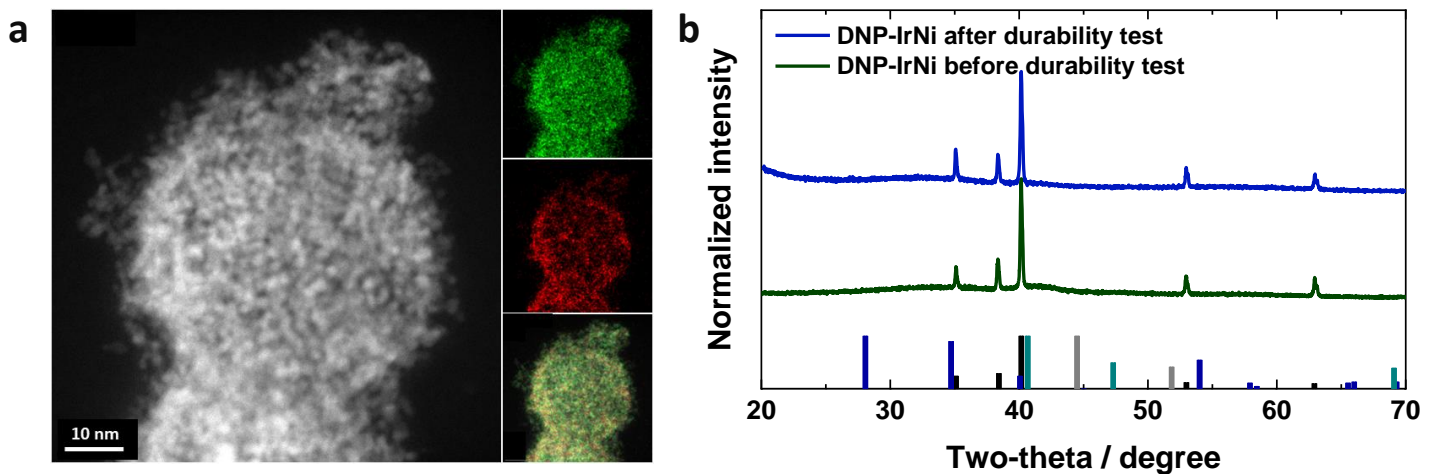


Figure S13. (a) STEM image with elemental mapping of DNP-IrNi after applying a constant current density of 100 mA cm^{-2} for 50 h. The colors indicate Ni (red) and Ir (green), (b) XRD patterns of DNP-IrNi before and after durability test at current density of 100 mA cm^{-2} for 50 h.

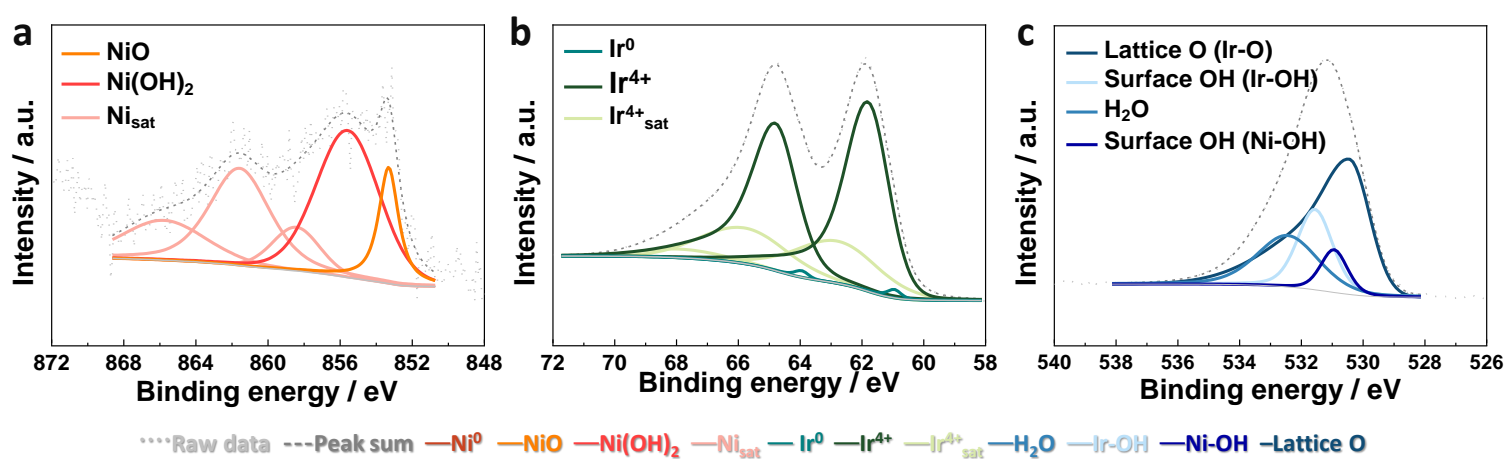


Figure S14. XPS spectra of (a) Ni 2p_{3/2}, (b) Ir 4f and (c) O 1s of DNP-IrNi after durability test at 100 mA cm⁻² for 50 h.

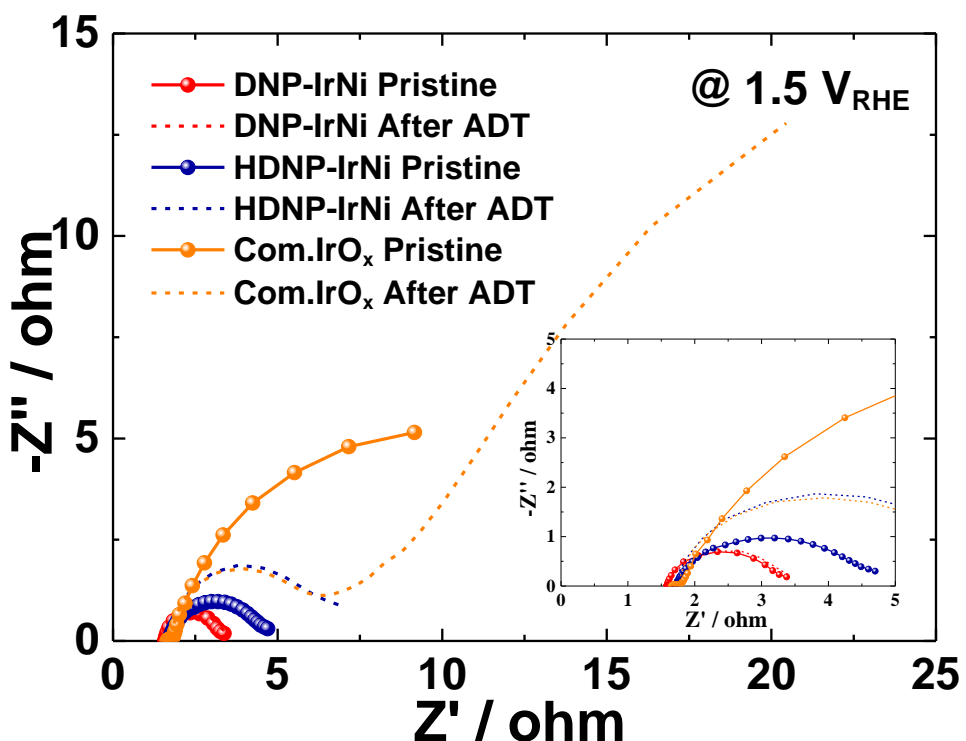


Figure S15. Electrochemical impedance spectroscopy measurement of DNP-IrNi, HDNP-IrNi and Com. IrO_x before and durability test at 100 mA cm^{-2} for 50 h.

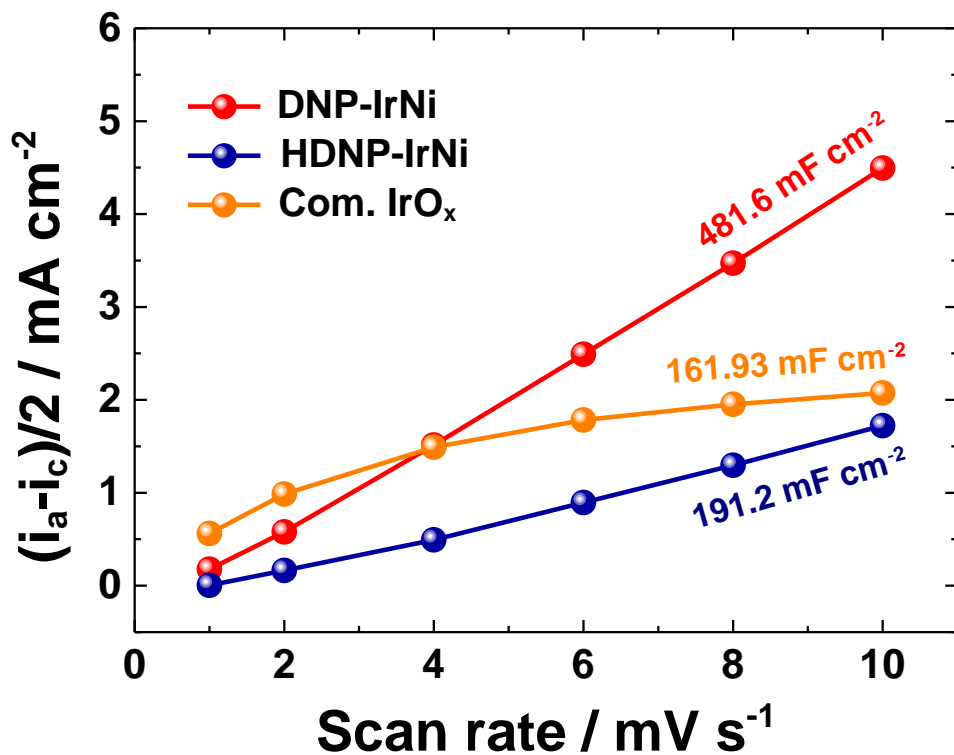


Figure S16. Measurements of electrochemical double layer capacitances of DNP-IrNi, HDNP-IrNi and Com. IrO_x after durability test at 100 mA cm^{-2} for 50 h.

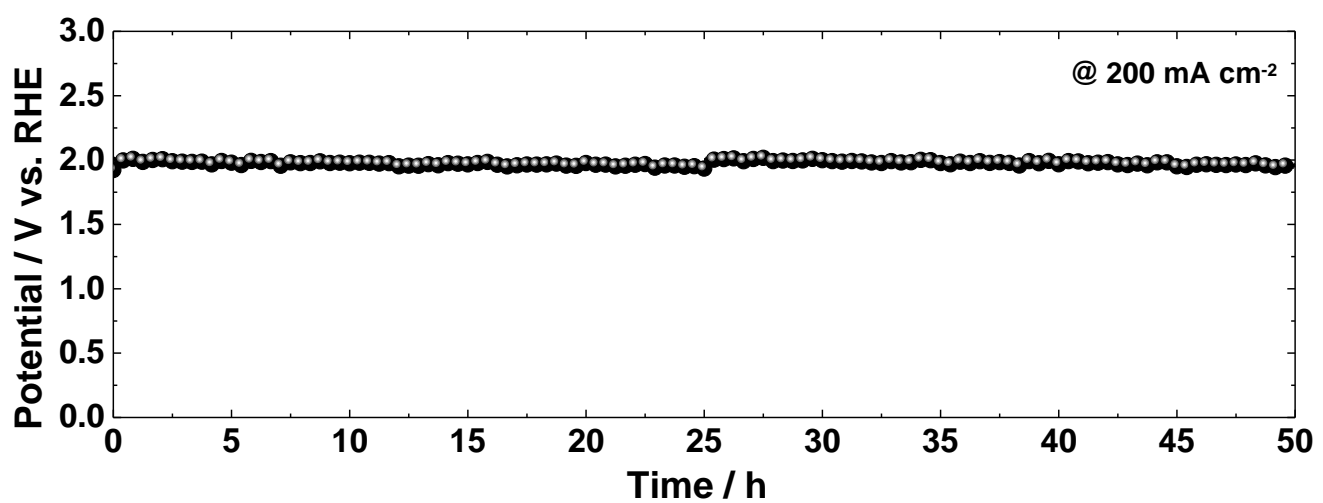


Figure S17. Durability test of DNP-IrNi at a constant current density of 200 mA cm^{-2} for 50 h (without iR compensation).

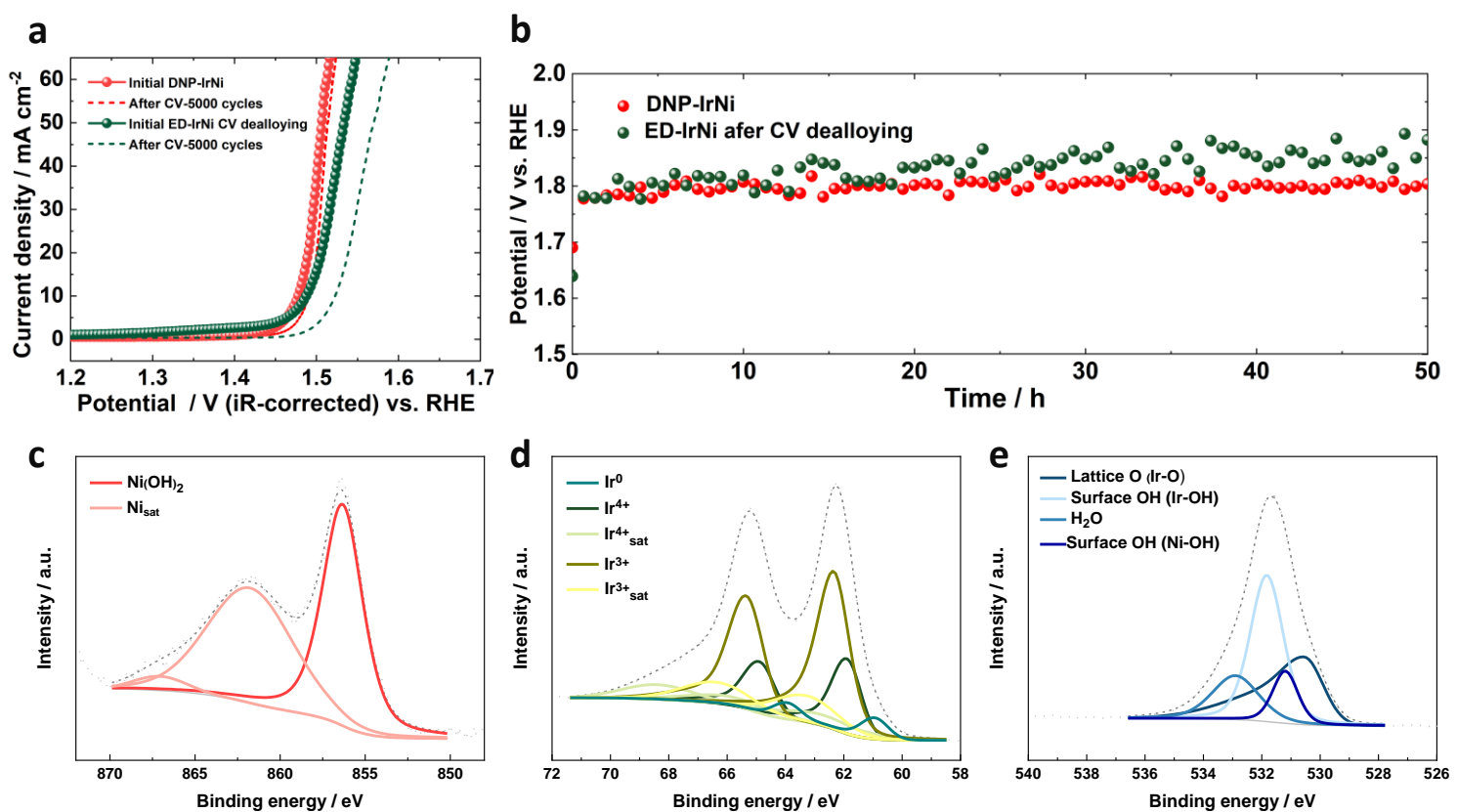


Figure S18. (a) OER polarization curve before and after accelerated degradation test (ADT) of DNP-IrNi and ED-IrNi after CV dealloying in the range of 1.2–1.6 V_{RHE} for 5000 cycles at a scan rate of 100 mV s⁻¹. (b) Chronopotentiometry at 100 mA cm⁻² for 50 h (without iR-compensation), XPS spectra of (c) Ni 2p_{3/2}, (d) Ir 4f and (e) O 1s of ED-IrNi after CV dealloying

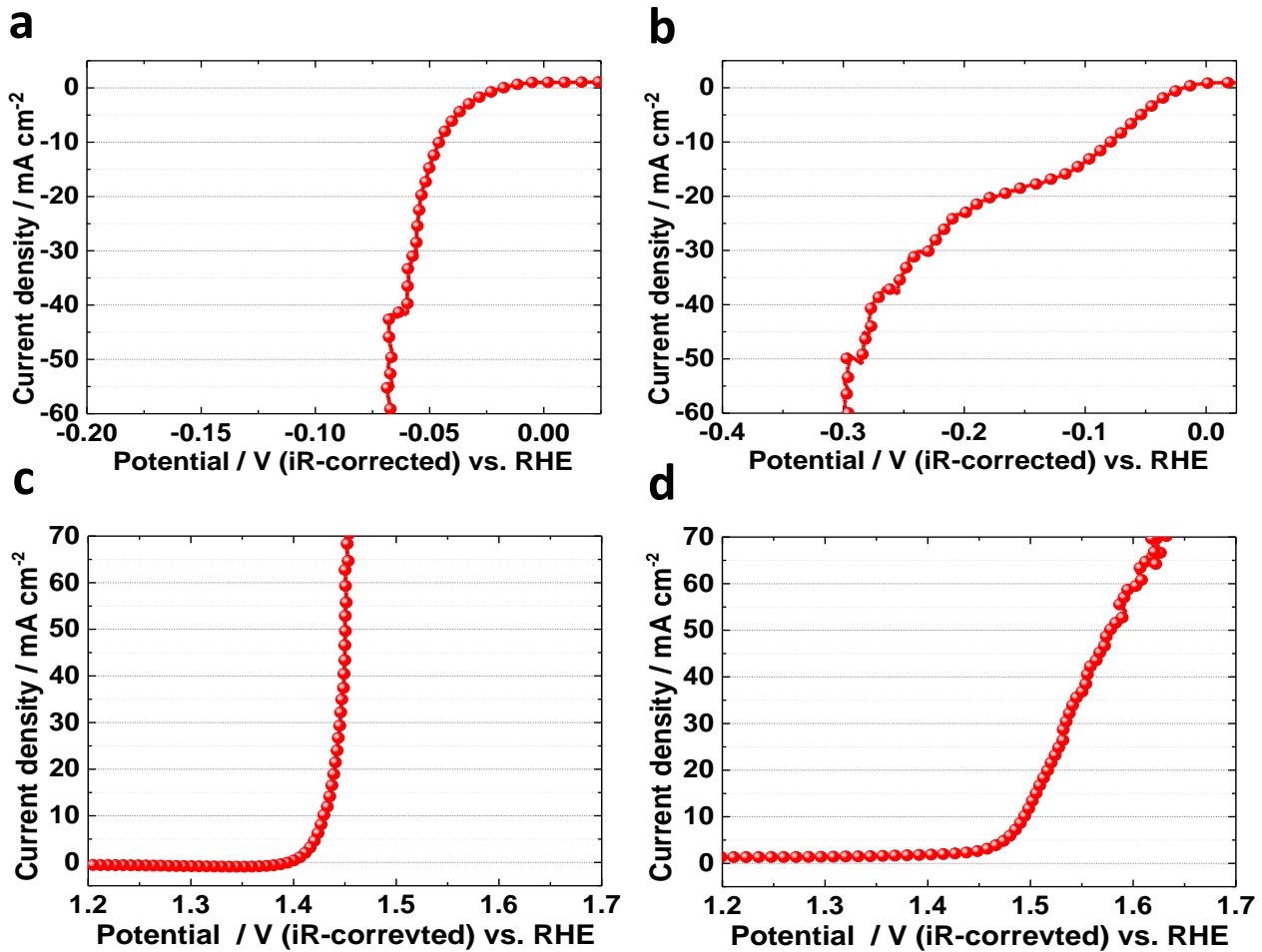


Figure S19. Polarization curves of DNP-IrNi for HER in (a) 1 M KOH solution (pH: 13.5) and (b) 1 M PBS solution (pH: 7.4), and for OER in (c) 1 M KOH solution and (d) 1 M PBS solution.

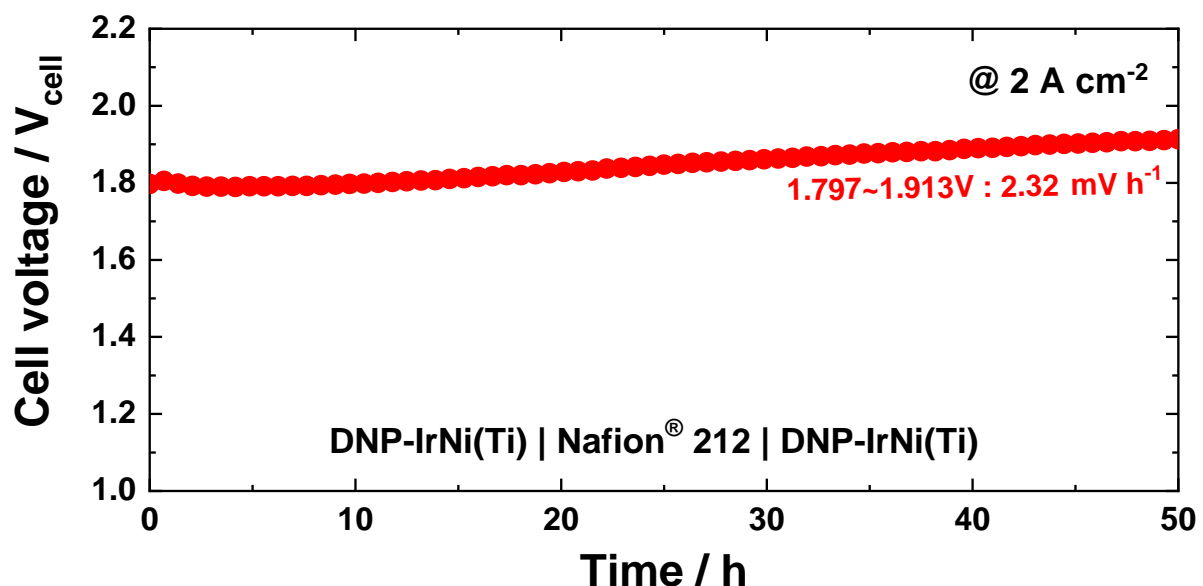


Figure S20. Durability test of DNP-IrNi(Ti) as bifunctional electrodes of PEMWE at a current density of 2 A cm^{-2} .

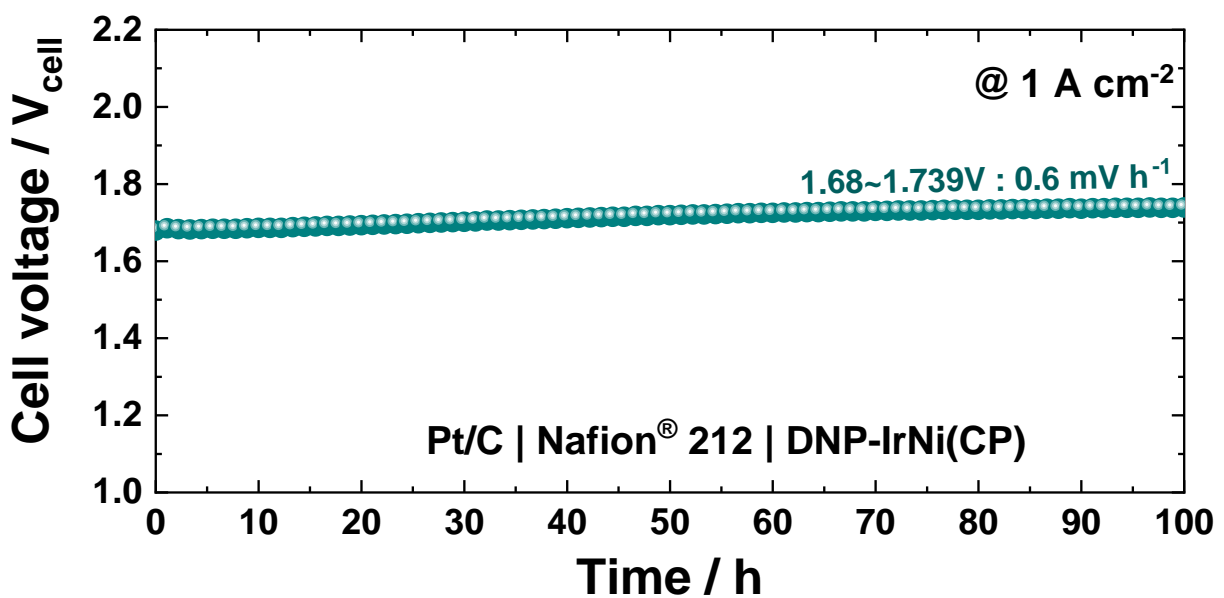


Figure S21. Durability test of DNP-IrNi(CP) as an anode of PEMWE at a current density of 1 A cm^{-2} .

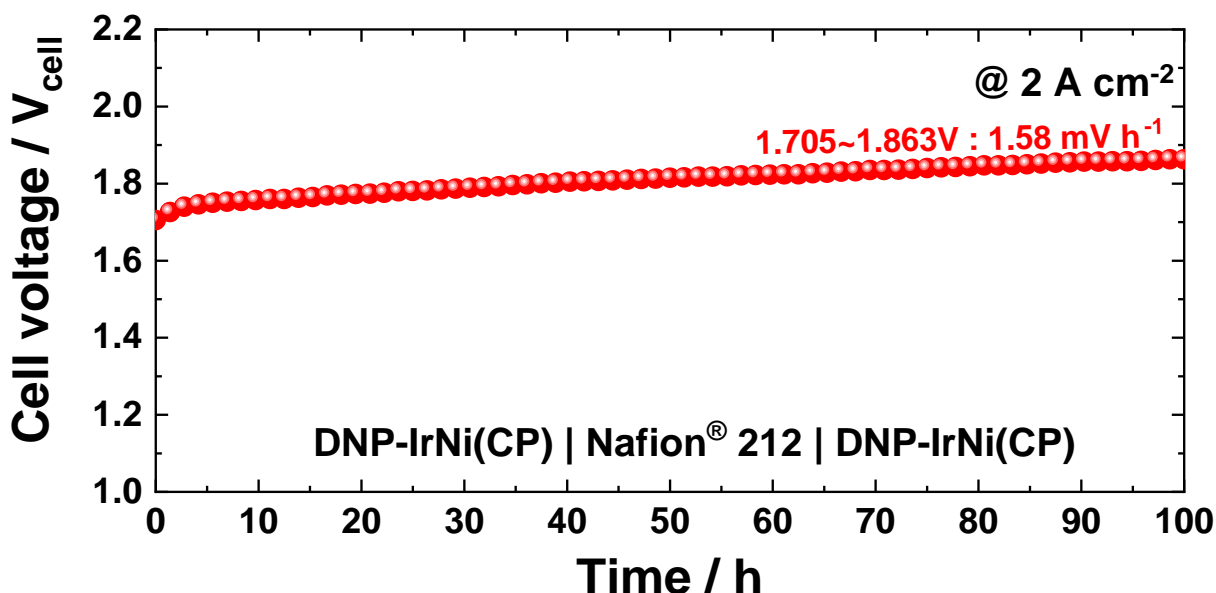


Figure S22. Durability test of DNP-IrNi(CP) as bifunctional electrodes of PEMWE at a current density of 2 A cm^{-2} .